Bull. Mater. Sci., Vol. 36, No. 3, June 2013, pp. 389–393. © Indian Academy of Sciences.

Effects of Bi doping on dielectric and ferroelectric properties of PLBZT ferroelectric thin films synthesized by sol–gel processing

HUA WANG[†,‡,*], **LI LIU**[†], **JI-WEN XU**[†,‡], **CHANG-LAI YUAN**[†,‡] **and LING YANG**[†]
[†]School of Materials Science and Engineering, [‡]Guangxi Key Laboratory of Information Materials, Guilin University of Electronic Technology, Guilin 541 004, China

MS received 21 November 2011; revised 31 July 2012

Abstract. **$[Pb_{0.95}(La_{1-y}Bi_y)_{0.05}][Zr_{0.53}Ti_{0.47}]O_3$ (PLBZT) ferroelectric thin films have been synthesized on indium tin oxide (ITO)-coated glass by sol–gel processing. PLBZT thin films were annealed at a relatively low temperature of 550 °C in oxygen ambient. Effects of Bi doping on structure, dielectric and ferroelectric properties of PLBZT were investigated. Bi doping is useful in crystallization of PLBZT films and promoting grain growth. When the Bi-doping content y is not more than 0·4, an obvious improvement in dielectric properties and leakage current of PLBZT was confirmed. However, when the Bi-doping content is more than 0·6, the pyrochlore phase appears and the remnant polarization P_r of PLBZT thin films is smaller than that of $(Pb_{1-x}La_x)(Zr_{1-y}Ti_y)O_3$ (PLZT) thin films without Bi doping. PLBZT thin films with excessive Bi-doping content are easier to fatigue than PLZT thin films.**

Keywords. **Ferroelectric thin film; $(Pb_{1-x}La_x)(Zr_{1-y}Ti_y)O_3$ (PLBZT); Bi doping; sol–gel.**

1. Introduction

Non-volatile memories occupy an increased share of the growing memory market and becoming an indispensable component of memory circuits (Scott 2005; Tang *et al* 2007). $(Pb_{1-x}La_x)(Zr_{1-y}Ti_y)O_3$ (PLZT) thin films are attracting much attention for their ferroelectric and optical applications such as ferroelectric random access memories, infrared sensors and electro-optic devices, due to their high optical transparency, outstanding ferroelectric and electro-optic properties (Gaidi *et al* 2004; Khodorov and Gomes 2006; Leclerc *et al* 2006; Singh *et al* 2008). However, PLZT thin films have a serious drawback i.e. they have low polarization retention and large leakage current, which enormously restrict their applications. Much work has been done in the past to study the effects of substitution in the Pb site of PZT, but not much work has been done to report the effect of double doping at the Pb site. The La–K double doping PZT (PLKZT) ceramics show that their transition temperature and related parameters of ferroelectric phase are slowly influenced by the double doping of La and K at the Pb site (Mal and Choudhary 1997). La–Cs double doping PZT (PLCZT) ceramics can undergo diffuse phase transition with higher Cs concentration and the pairs of doping at the Pb sites created more structural disorder in PZT (Choudhary and Mal 2002). Goel *et al* (2004) and Goel and Yadav (2007) have reported that the La–Bi double doping PZT (PLBZT) ceramics have a significant effect on the dielectric properties of PZT system. Shannigrahi *et al* (1999, 2002) reported that the La–Li double doping PZT (PLLZT) thin films sol–gel-grown on $Pt/Ti/SiO_2/Si$ substrates exhibited fatigue-free behaviour up to $6{\cdot}5 \times 10^{10}$ switching cycles and have high dielectric constant of 10^4 and remnant polarization of 14–24 $\mu C/cm^2$.

Ferroelectric thin films were usually deposited on $Pt/Ti/SiO_2/Si$ substrates. For the optical–electrical application, substrate-coated transparent oxide electrodes are needed. Glass substrate coated indium tin oxide (ITO) is a good choice, since it has been widely applied in manufacture of transparent conductors and depositing PLZT ferroelectric films (Zheng *et al* 2005; Yoon *et al* 2008; Pak *et al* 2010). High annealing temperature is another problem in PLZT thin films synthesized on ITO-coated glass because common glass softens at high temperature. However, previous studies reported that annealing temperature higher than 600 °C is required to synthesize PLZT thin films (Khodorov and Gomes 2006; Singh *et al* 2008; Yoon *et al* 2008).

In this paper, synthesis and characterization of Bi-doping PLBZT thin films on ITO-coated glass substrates through sol–gel process is described. Effects of Bi doping on structure, dielectric and ferroelectric properties have been investigated.

2. Experimental

Prior to being coated, ITO-coated glass substrates were ultrasonically cleaned in distilled water, acetone and methanol.

*Author for correspondence (wh65@tom.com)

Lead acetate (excess 10% to compensate the lead loss during annealing process), zirconium nitrate, lanthanum nitrate and bismuth nitrate were dissolved, respectively, in 2-methoxyethanol at 80 °C and dehydrated at 120 °C. Then, tetra-butyl titanate was dissolved in acetylacetone and 2-methoxyethanol at 40 °C. The spin-on technique was employed to deposit solution on ITO-coated glass substrates. After spinning onto substrates, wet films were kept on a hot plate in air at 300 °C for 10 min to remove solvents and other organics. The desired thickness of PLBZT thin films was achieved by multiple spin-bake processes. The dry multilayer films were annealed for 30 min at 550 °C in oxygen ambient.

For determination of electrical properties, capacitors were formed by sputtering platinum (Pt) electrodes of 0·1 mm diameter through a shadow mask on PLBZT films. The phase structure of films was analysed by X-ray diffraction (XRD), ferroelectric behaviour was determined using ferroelectric tester (Radiant P-WS), dielectric properties of films were measured using an impedance analyser (Agilent 4294A) and leakage current measurements were performed using source meter (Keithley 4200).

3. Results and discussion

Figure 1 shows XRD patterns of $[Pb_{0.95}(La_{1-y}Bi_y)_{0.05}][Zr_{0.53}Ti_{0.47}]O_3$ (PLBZT, $y = 0{\cdot}2$, 0·4, 0·6 and 0·8) and PLZT ($y = 0{\cdot}0$) thin films. It can be seen that the locations of the peaks in XRD patterns of all samples are coincident, which indicate that there are no distinct differences in phase structure of PLZT and PLBZT thin films with different Bi-doping contents. When the Bi-doping content is not more than 0·6, PLBZT films are well-crystallized and exhibit a polycrystalline perovskite phase structure, with no pyrochlore phase, which is similar to the phenomenon from earlier research on PLBZT ceramics by Goel *et al* (2004). On increasing Bi-doping content from 0·1 to 0·4, reflection peaks become sharp and reflection intensities also increase, which indicate that Bi doping is useful in the crystallization of PLBZT films and promoting grain growth. But then, some reflection peaks such as (111) and (200) are suppressed when the Bi-doping content is more than 0·4, which may be due to the structural disorder derived from the Bi^{3+} entering the B-site to replace Ti^{4+} or Zr^{4+}. Furthermore, when the Bi-doping content is more than 0·6, the peaks of the pyrochlore phase appear. In addition, a slight shift of characteristic peaks in XRD patterns of PLBZT films is observed, this suggests that La ions in the lattice were partly replaced by smaller Bi ions and then decrease the lattice constant.

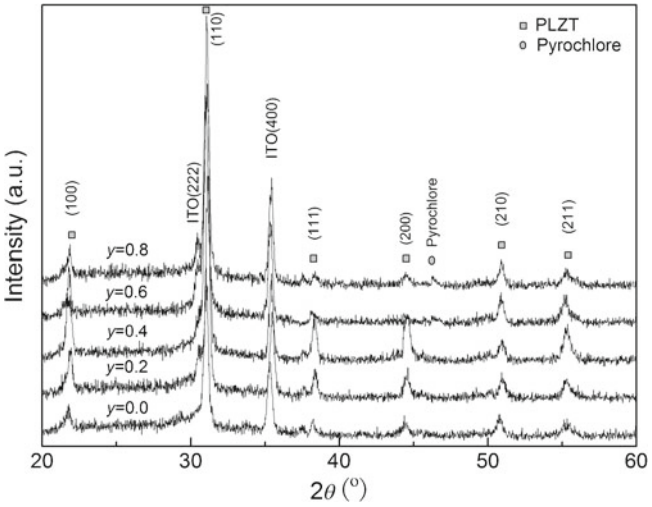

Figure 1. XRD patterns of $[Pb_{0.95}(La_{1-y}Bi_y)_{0.05}][Zr_{0.53}Ti_{0.47}]O_3$ thin films.

The surface morphology and cross-section SEM photographs of PLBZT thin films with various Bi-doping contents are shown in figure 2. Dense, smooth and crack-free surface morphologies can be observed in all the films. With the increase in Bi-doping content from 0·2 to 0·6, average grain size was obviously increased from about 50 nm in figure 2(a) to 100 nm in figure 2(c). Besides, it can also be seen that there is a clear boundary between PLBZT film and ITO-coated glass substrate in figure 2(d), which means that the interaction and interdiffusion between PLBZT films and ITO-coated glass substrates is inconspicuous.

Figure 3 shows polarization–electric field (P–E) hysteresis curves of PLZT and PLBZT (Bi-doping content, $y = 0{\cdot}6$) thin films, measurement with the structure of Pt/PLZT/ITO and Pt/PLBZT/ITO, respectively. As shown in figure 3, well-saturated hysteresis loops and almost the same values of coercive field, E_c, are observed in PLZT ($y = 0$) and PLBZT ($y = 0{\cdot}6$) thin films, but the remnant polarization, P_r value in PLBZT ($y = 0{\cdot}6$) thin films is smaller than that of PLZT ($y = 0$) thin films. Furthermore, it can be seen that the P–E curves do not show any noticeable asymmetric behaviour resulting in imprint failures. Figure 4 is the remnant polarization, P_r and coercive field, E_c of PLBZT thin films as a function of Bi-doping content. From figure 4, it can be seen that the P_r and E_c of PLBZT thin films are strongly dependent on the Bi content, y. The remnant polarization, P_r, retains almost the same value of 25 $\mu C/cm^2$ with increase in Bi-doping content from 0·2 to 0·4, then decreased drastically with the increasing Bi-doping content over 0·6. Meanwhile, the coercive field, E_c, decreased slowly with the increase in Bi-doping content from 0·2 to 0·4, then increased slightly. The radius of Bi^{3+} (0·103 nm) is close to that of La^{3+} (0·106 nm) and it is quite probable that the Bi ions enter La ions simultaneously, thereby, the strength of spontaneous polarization does not change obviously. However, the radius of Bi^{3+} is much closer to that of Ti^{4+} (0·0605 nm) or Zr^{4+} (0·072 nm) and can also replace the B-site in perovskite PZT lattice confirmed by Goel *et al* (2004). With the increase in Bi-doping content, some Bi^{3+} enter the B-site to replace Ti^{4+} or Zr^{4+}, the substitution disorder in the arrangement of cations in one or more crystallographic sites of the structure results in increase in domain

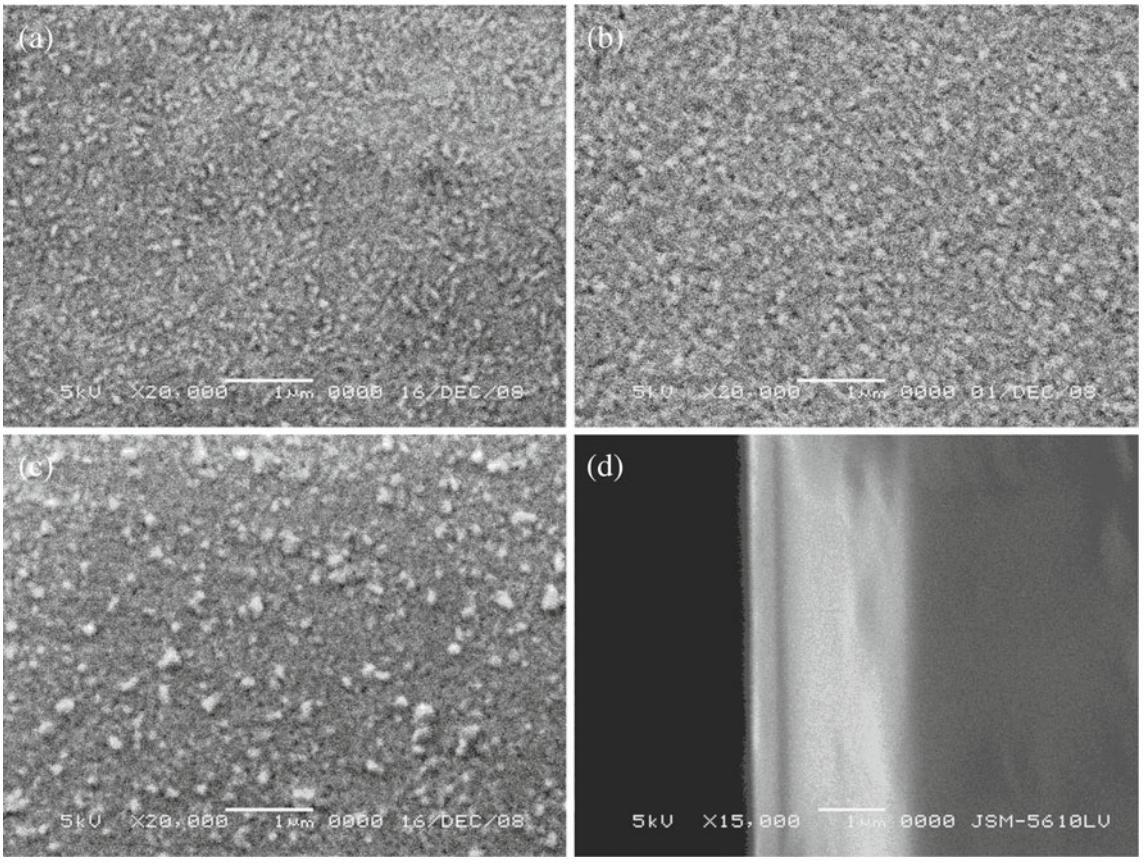

Figure 2. SEM images of $[Pb_{0.95}(La_{1-y}Bi_y)_{0.05}][Zr_{0.53}Ti_{0.47}]O_3$ thin films with various Bi-doping contents, y. (**a**) $y = 0.2$, (**b**) $y = 0.4$, (**c**) $y = 0.6$ and (**d**) cross-sectional morphology.

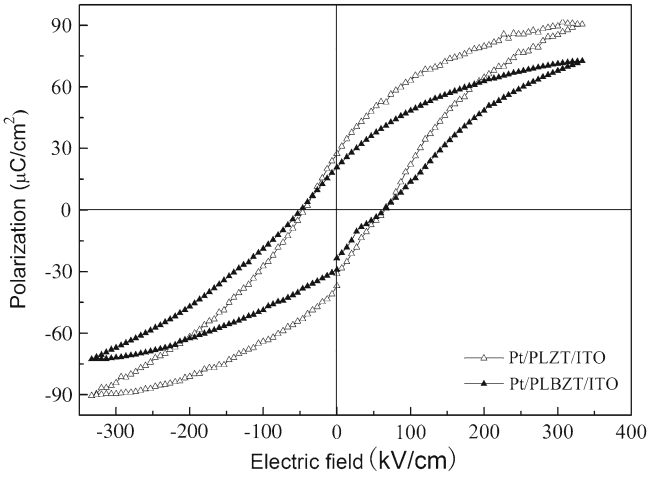

Figure 3. *P–E* hysteresis curves of PLZT and PLBZT (Bi-doping content, $y = 0.6$) thin films.

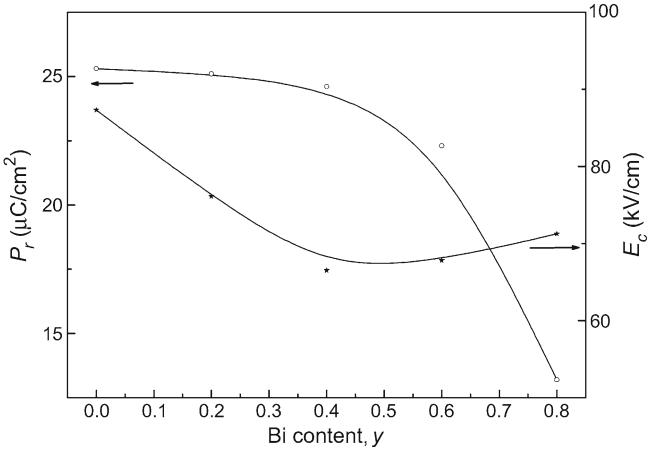

Figure 4. P_r and E_c of $[Pb_{0.95}(La_{1-y}Bi_y)_{0.05}][Zr_{0.53}Ti_{0.47}]O_3$ thin films with various Bi contents, y.

wall mobility, thereby, both the strength of polarization and coercive field decrease.

The polarization decays of PLZT and PLBZT thin films were studied from the structures of Pt/PLZT/ITO and Pt/PLBZT/ITO (Bi-doping content, $y = 0.6$), respectively by applying 10 kHz bipolar pulses of 5 V amplitude. Figure 5 represents normalized polarizations of PLZT and PLBZT thin films as a function of switching cycles. In both the cases, films exhibit an identical trend in fatigue behaviour. In the initial long period (up to about 10^8 cycles for PLZT and 10^7 cycles for PLBZT), the P_r is almost constant, which

is then followed by a final decay period. Even after 10^9 switching cycles, the decay in P_r of PLZT is only 10% of the initial value; on the other hand, the same decay of P_r occurs in PLBZT thin films only after 10^8 switching cycles. These suggest that the PLBZT thin films with excessive Bi-doping content are easier to fatigue than PLZT thin films. Compared with the fatigue characteristics of the $Pt/Pb_{0.98}(La_{1-x}Li_x)_{0.02}(Zr_{0.55}Ti_{0.45})O_3/Pt$ (Pt/PLLZT/Pt) capacitor (Shannigrahi *et al* 2002), this is not a significant improvement. It is known that oxygen vacancy is one of the primary causes of fatigue behaviour, thus the observed fatigue characteristics in PLBZT seem to be closely related to the reduced concentration of oxygen vacancies which is less than that in PLLZT.

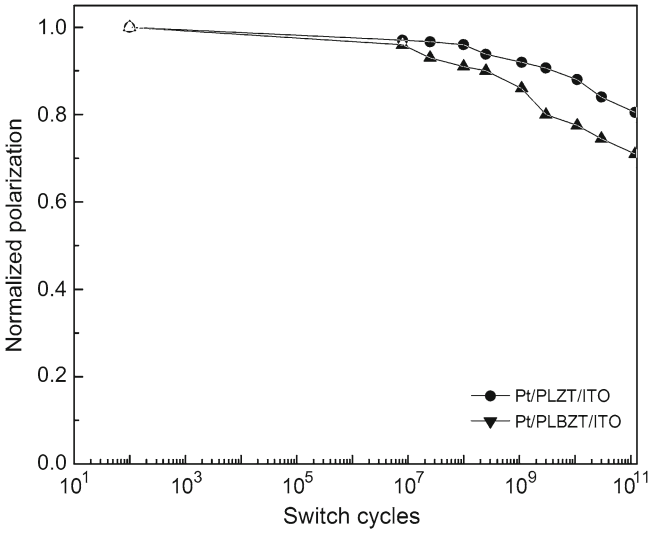

Figure 5. Decay in normalized polarization of PLZT and PLBZT (Bi-doping content, $y = 0{\cdot}6$) thin films as a function of switching cycles.

Figure 6 shows dielectric constant and dielectric loss of PLBZT films with various Bi-doping contents at 200 kHz. From figure 6, it can be seen that the dielectric constant, ε_r, of PLBZT films first increases, then decreases with the increase in Bi-doping content. When the Bi-doping content y is 0·4, ε_r reaches the largest value of about 770, which is larger than that of PLZT ($y = 0$) thin films without Bi-doping. The varying trend in dielectric loss tan δ of PLBZT is in contrast to the dielectric constant, ε_r. It has been established that ε_r decreases with decreasing grain size, the increase in ε_r and decrease in tan δ of PLBZT; with the increase in Bi-doping content from 0·2 to 0·6 is mainly ascribed to the increasing grain size observed in figure 2. However, the structural disorder which is derived from the super-abundant Bi doping will result in decrease in ε_r and increase in tan δ.

A noticeable improvement in leakage current can be confirmed from figure 7. It can be seen that the leakage currents in all samples of PLBZT thin films are lower than 10^{-8} Å at a voltage of 5 V and these leakage currents are all very much smaller than that of PLZT thin films without Bi. The lowest leakage current value of $2{\cdot}3 \times 10^{-9}$ Å can be observed in PLBZT thin films when the Bi-doping content is 0·4. Nevertheless, as the Bi-doping content is more than 0·4, leakage current in PLBZT will increase slightly again, in which the varying trend is in contrast to that of dielectric constant for PLBZT thin films. This increase in leakage current may be related to the existence of the pyrochlore phase, which will increase the interface states and defect concentration. Besides, it can be seen that leakage current characteristics of PLBZT films at positive electric field and negative electric field regions are similar as shown in the inset curve in figure 7. There are two regions of linear increase and exponential increase. The linear increase of leakage current at lower voltage implies that the conductive

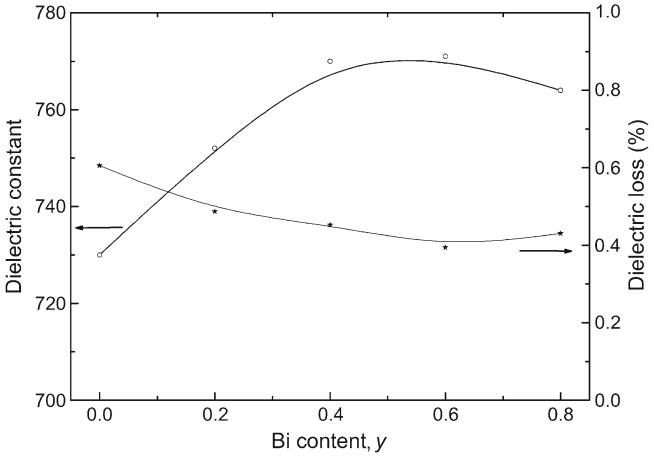

Figure 6. Dielectric constant and dielectric loss of $[Pb_{0.95}(La_{1-y}Bi_y)_{0.05}][Zr_{0.53}Ti_{0.47}]O_3$ thin films with various Bi-doping contents, y.

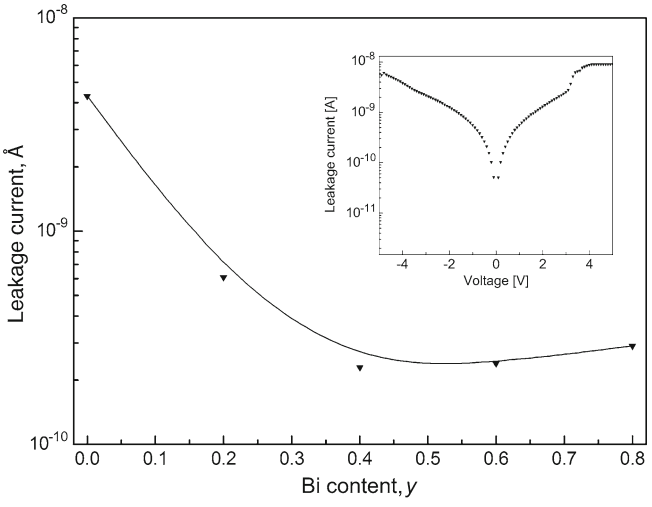

Figure 7. Leakage currents of $[Pb_{0.95}(La_{1-y}Bi_y)_{0.05}][Zr_{0.53}Ti_{0.47}]O_3$ thin films and I–V curve of PLBZT with Bi-doping content, $y = 0{\cdot}4$.

mechanism is Ohm conduction and the exponential increase of leakage current at higher voltage suggests that the conductive mechanism is Schottky emission. However, slight asymmetry of the I–V characteristic may be attributed to the difference between Pt top electrode and ITO bottom electrode.

4. Conclusions

The Bi-doping of PLBZT thin films can be synthesized by sol–gel processing at a relatively low annealing temperature of 550 °C in oxygen ambient. Bi-doping is useful in crystallization of PLBZT films and promoting grain growth. However, when the Bi-doping content is more than 0·6, the pyrochlore phase appears and the remnant polarization, P_r, of PLBZT thin films is smaller than that of PLZT thin films without Bi doping. P_r and E_c of PLBZT thin films are strongly dependent on the Bi-doping content, y, P_r retains almost the same value of 25 $\mu C/cm^2$ with the increase in Bi-doping content from 0·2 to 0·4, then decreases drastically. PLBZT thin films with excessive Bi-doping content are easier to fatigue than PLZT thin films. When the Bi-doping content, y, is not more than 0·4, dielectric properties, ε_r, decrease to the largest value of about 770 with increase in Bi-doping content, which is larger than that of PLZT thin films without Bi-doping. The lowest leakage current value of $2{\cdot}3 \times 10^{-9}$ Å can be observed in PLBZT thin films when the Bi-doping content is 0·4, which is much smaller than that of PLZT thin films without Bi doping.

Acknowledgements

This work was supported by the Science Foundation of Guangxi (Grant No. 0832247) and the Guangxi Specific Project Construction of Infrastructure Platform for Science and Technology (Grant No. 10-046-13).

References

Choudhary R N P and Mal J 2002 *Mater. Sci. Eng.* **B90** 1
Gaidi M, Amassian A, Chaker M, Kulishov M and Martinu L 2004 *Appl. Surf. Sci.* **226** 347
Goel P and Yadav K L 2007 *J. Mater. Sci.* **42** 3928
Goel P, Yadav K L and James A R 2004 *J. Phys. D: Appl. Phys.* **37** 3174
Khodorov A and Gomes M J M 2006 *Thin Solid Films* **515** 1782
Leclerc G, Domenges B, Poullain G and Bouregba R 2006 *Appl. Surf. Sci.* **253** 1143
Mal J and Choudhary R N P 1997 *J. Phys. Chem. Solids* **58** 421
Pak J, Park S, Nam K and Park G 2010 *Thin Solid Films* **518** 5642
Scott J F 2005 *Mater. Sci. Eng.* **B120** 6
Shannigrahi S R, Choudhary R N P, Acharya H N and Sinha T P 1999 *J. Appl. Phys.* **85** 1713
Shannigrahi S R, Lee S H and Jang H M 2002 *J. Am. Ceram. Soc.* **85** 2122
Singh R, Goel T C and Chandra S 2008 *Mater. Res. Bull.* **43** 384
Tang M H, Zhou Y C, Zheng X J, Yan Z, Cheng C P, Ye Z and Hu Z S 2007 *Solid State Electron.* **51** 371
Yoon J E, Cha W H, Lee I S, Kim S J and Son Y G 2008 *Surf. Coat. Technol.* **203** 638
Zheng F G, Chen J P, Li X W and Shen M R 2005 *Mater. Lett.* **59** 3498